Effect of carbon decoration on the absorption of ⟨100⟩ dislocation loops by dislocations in iron

2014 J. Phys.: Condens. Matter 26 165402

(http://iopscience.iop.org/0953-8984/26/16/165402)

IOP Publishing Journal of Physics: Condensed Matter
J. Phys.: Condens. Matter **26** (2014) 165402 (10pp) doi:10.1088/0953-8984/26/16/165402

Effect of carbon decoration on the absorption of ⟨1 0 0⟩ dislocation loops by dislocations in iron

D Terentyev[1], A Bakaev[1,2,3] and E E Zhurkin[3]

[1] SCK•CEN, Nuclear Materials Science Institute, Boeretang 200, Mol, B2400, Belgium
[2] Center for Molecular Modeling, Department of Physics and Astronomy, Ghent University, Technologiepark 903, 9052 Zwijnaarde, Belgium
[3] Department of Experimental Nuclear Physics, Institute of Physics, Nanotechnologies and Telecommunications, St Petersburg State Polytechnical University, 29 Polytekhnicheskaya str., 195251, St Petersburg, Russia

E-mail: dterenty@sckcen.be

Received 27 October 2013, revised 6 February 2014
Accepted for publication 7 February 2014
Published 1 April 2014

Abstract
This work closes a series of molecular dynamics studies addressing how solute/interstitial segregation at dislocation loops affects their interaction with moving dislocations in body-centred cubic Fe-based alloys. We consider the interaction of ⟨1 0 0⟩ interstitial dislocation loops decorated by different numbers of carbon atoms in a wide temperature range. The results reveal clearly that the decoration affects the reaction mechanism and increases the unpinning stress, in general. The most pronounced and reproducible increase of the unpinning stress is found in the intermediate temperature range from 300 up to 600 K. The carbon-decoration effect is related to the modification of the loop–dislocation reaction and its importance at the technologically relevant neutron irradiation conditions is discussed.

Keywords: dislocation, carbon, iron, segregation

S Online supplementary data available from stacks.iop.org/JPhysCM/26/165402/mmedia

(Some figures may appear in colour only in the online journal)

1. Introduction

Body-centred cubic iron (bcc Fe) is one of the most important technological metals especially for structural applications, including nuclear sector. Fe–chromium–carbon-based ferritic and ferritic/martensitic (F/M) steels are promising candidate structural materials for Fusion and GEN IV nuclear reactors [1]. Nevertheless they suffer from severe degradation of mechanical properties when exposed to neutron irradiation at reactor operation temperature in terms of hardening, loss of ductility and finally embrittlement [1]. Moreover, once a relatively high level of radiation-induced hardening is reached, the work hardening measured in uniaxial tensile tests becomes either strongly reduced or even inexistent [2–4]. The latter phenomenon is called plastic-induced softening or instability and it is considered as a potentially serious problem in the assessment of the integrity of components made with steels and subjected to high neutron dose.

The physical origin of the hardening and change of plastic behaviour of neutron irradiated Fe (and metals in general) lays in the formation of nano-scale agglomerates being clusters of point defects which obstruct dislocation movement [5]. Agglomeration of vacancies results in the formation of nano-voids, while gathering of self-interstitial atoms (SIAs) leads to the formation of platelet clusters known as dislocation loops [6]. Self-interstitials and vacancies are produced in neutron-induced collision cascades in equal amounts. However, the growth of voids and SIA clusters occurs at different rates, depending on irradiation conditions and material. In the case of bcc Fe and Fe-based ferritic steels, the dislocation loops are recognized as the primary neutron-induced nano-structural defects. Hence, the degradation of the mechanical response is

primarily related to the accumulation and growth of dislocation loops [7–11]. This is why the complete understanding of the interaction of dislocations with dislocation loops, i.e. reaction mechanism and unpinning stress, is an important subject. Moreover, the plastic instability phenomenon, mentioned earlier, is currently understood to be a consequence of the removal of the dislocation loops by moving dislocation lines. This process can explain the formation of clear bands or dislocation channels, seen by transmission electron microscopy, that make the material locally inhomogeneous and unstable upon load [12]. Clear bands in pure Fe [8] and modifications of loop pattern in Fe–9Cr [7] have been experimentally observed.

To rationalize the formation of clear bands in bcc Fe, molecular dynamics (MD) modelling was applied to address the interaction of moving dislocations with dislocation loops [13–18]. The absorption of dislocation loops was explained on the basis of reactions between different dislocation segments observed using dislocation-core analysis in atomistic simulations. The principal mechanisms ensuring loop absorption were determined to be same for both screw and edge dislocations, irrespective of the interaction occurring with ½⟨1 1 1⟩ or ⟨1 0 0⟩ loops. Importantly, the absorption process was found to be enhanced by increasing temperature. The role of thermal activation and the competition between different reaction pathways (leading to loop absorption or structural transformation) was also identified with the aid of MD simulations [19, 20]. By transferring the MD results to a dislocation dynamics approach, it became possible to assess simultaneously the role of thermal activation in hardening and, if needed, to introduce a numerical criterion for loop absorption or structural transformation implicitly treating loops as stochastic obstacles [21]. The good agreement between experiment and modelling for the strengthening due to ½⟨1 1 1⟩ loops in bcc Fe has shown the adequacy and usefulness of such MD simulations. The formation of dislocation channels upon plastic deformation of Fe containing ½⟨1 1 1⟩ loops has been also explained on the basis of rigorous dislocation dynamics simulations treating loops as dislocation segments [22].

Real F/M steels, however, contain a set of alloying elements among which the most important are substitutional chromium (Cr) and interstitial carbon (C). Two types of interstitial dislocation loops with Burgers vector (BV) ½⟨1 1 1⟩ and ⟨1 0 0⟩ are known to form in high Cr steels, with the fraction being dependent on Cr content [23, 24] and irradiation temperature [25]. More recently, fine atom probe and transmission electron microscopy (TEM) experiments unambiguously revealed Cr and C segregation to dislocation loops in model Fe–Cr alloys as well as in commercial F/M steels [26, 27]. Taking into account this evidence, recent MD studies have addressed the effect of Cr and C segregation on ½⟨1 1 1⟩ loops and ⟨1 0 0⟩ loops [28–30]. In the case of ½⟨1 1 1⟩ loops, it was demonstrated that Cr or C segregation modifies the interaction mechanism and increases the unpinning stress depending on ambient temperature and loop size. However, the effect of carbon decoration on the resistance of ⟨1 0 0⟩ loops, observed in bcc Fe, Fe–C and Fe–Cr alloys, as well as in F/M steels, upon irradiation at elevated temperature, has not been studied so far, while there is evidence of strong interaction of C with ⟨1 0 0⟩ loops [31].

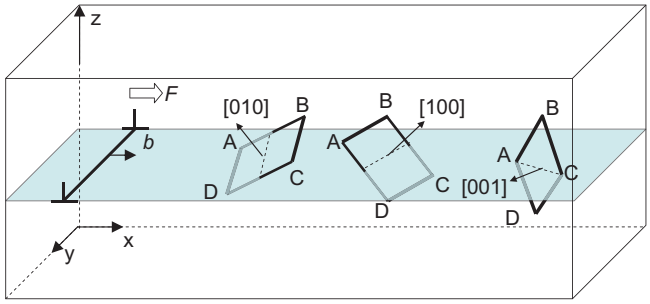

Figure 1. Interaction geometry for three possible orientations of ⟨1 0 0⟩ loops interacting with a ½⟨1 1 1⟩⟨1 1 0⟩ edge dislocation.

This work closes therefore a series of MD studies dedicated to the effect of Cr–C segregation on the interaction with gliding dislocations [28–30]. Since the previous works addressing the interaction of dislocation defects in Fe considered a ½⟨1 1 1⟩⟨1 1 0⟩ edge dislocation, we continue the investigation using the same type of dislocation. Here, we consider the interaction of ⟨1 0 0⟩ interstitial dislocation loops with size 3.5 nm being decorated by different amount of C atoms. The paper is organized as follows. First we present the background in terms of the analysis of loop–dislocation interactions in the absence of C decoration. Then, the MD computational details are briefly described. The results are subdivided into two sections separately addressing the effect of C decoration on the reaction mechanisms and unpinning stress. The paper closes with discussion and conclusions.

2. Background: interaction mechanisms in pure Fe

Prior to describing the computational methodology and results, we summarize the interaction mechanisms operating for ⟨1 0 0⟩ loops in Fe. For each interaction geometry we provide a schematic picture that shows the elementary steps constituting the interaction processes, which will be useful for describing the effects of C decoration.

There are three possible orientations of a ⟨1 0 0⟩ dislocation loop with respect to a ½[1 1 1] ($\bar{1}$1 0) edge dislocation, which are shown in figure 1. In this work, we consider square loops with sides oriented along ⟨1 0 0⟩ directions, as observed in experiments in pure Fe under ion irradiation [25]. The dashed lines crossing the loop's surfaces in figure 1 indicate the intersection with the dislocation glide plane (DGP). The corners of the loops are labelled by letters to facilitate description of the reactions. *x*, *y* and *z* axes on the figure correspond to [1 1 1], [1 1 $\bar{2}$] and [$\bar{1}$1 0] directions, respectively. In the following we list the typical interaction mechanisms observed for the undecorated loops, previously presented in [17].

(a) We shall start the description of the mechanisms from the case of $\boldsymbol{b}_L$= [1 0 0]. The interaction details are shown schematically in figure 2 (see also animated gif figure 2 attached as online supplementary materials (stacks.iop.org/JPhysCM/26/165402/mmedia). The dislocation line glides towards the loop and forms a reaction segment (RS) of ½[1 1 1] type on contact (see figure 2(*b*)). The RS, which is not glissile in the DGP, pins the dislocation.

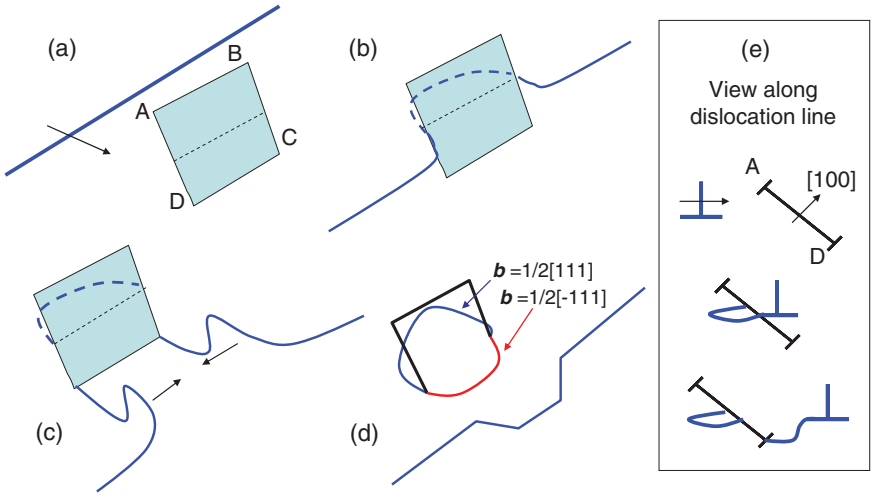

Figure 2. Schematic representation of the interaction mechanism for a loop with $\boldsymbol{b}_L = [1\,0\,0]$ at low temperature, $T \leq 150$ K.

At 150 K and below, the loop is simply sheared by the dislocation. At 300 K, the unpinning proceeds with the formation of a screw dipole, cross-slip of dislocation arms along sides AB and BC (see figures 2(*c*) and (*e*)) and their closure. The so called 'bi-loop' formed by a set of [1 0 0]; ½ [$\bar{1}$ 1 1] and ½ [1 1 1] segments is left behind (see figure 2(*d*)).

In high temperature (300–600 K) simulations, the upper segment 'AB' (see figure 1) is always seen to 'flip' on the glide plane. The interaction details are presented schematically in figure 3 (figures 3(*a*) and (*b*); see also animated gif figure 3 stacks.iop.org/JPhysCM/26/165402/mmedia). This movement can be also interpreted as dissociation of [1 0 0] into two segments: ½[$\bar{1}\bar{1}\bar{1}$] and ½[$\bar{1}$ 1 1]. This reaction is unfavourable and therefore for it to occur the system must overcome a certain barrier. This is why such 'flip' is seen only at high enough temperature. As a result of the dissociation, the ½[$\bar{1}\bar{1}\bar{1}$] segment annihilates with the pre-existing ½[1 1 1] segment, while the ½[$\bar{1}$ 1 1] segment displaces underneath the DGP (see figure 3(*c*)). Thus, the remaining lower half of the [1 0 0] loop pins the dislocation. With increase of stress, the [1 0 0] segment DC propagates downwards reacting with the ½[$\bar{1}$ 1 1] segment and forming a superjog of ½[1 1 1] type on the dislocation line (see figures 3(*d*) and (*e*)). This configuration is glissile and the jogged dislocation advances under the action of shear stress.

The flipping of the upper part of the loop is found to be enhanced by increasing temperature. It is important to note that, in this configuration, the flip is not favoured due to the repulsion between upper dislocation loop segment and dislocation line. While in the configuration with $\boldsymbol{b}_L = [0\,1\,0]$, the upper side BC (see figure 1) is attracted to the dislocation line and the flipping movement is therefore favoured.

(b) The interaction details for the loop with $\boldsymbol{b}_L = [0\,1\,0]$ are given in figure 4 (see also animated gif figure 4 stacks.iop.org/JPhysCM/26/165402/mmedia). Upon contact with the dislocation line (figure 4(*b*)), the upper half of the loop flips on the DGP (see figure 4(*c*)) and is converted into ½[1 $\bar{1}$ 1] orientation. The latter segment immediately slips underneath the DGP and the lower [1 0 0] AD segment now acts as a lock (see figure 4(*d*)). The unpinning occurs by the glide of the AD segment across the part with BV ½[1 1 1], thereby converting the whole loop into a double superjog segment with $\boldsymbol{b}$ = ½[1 1 1] (see figure 4(*e*)). The last step of the reaction is just the same as in the reaction with a ½ [1 $\bar{1}$ 1] loop. The details of this process are shown in figure 2 in [17]. τ_C for the [0 1 0] loop is, however, much smaller than in the case of the ½ [1 1 1] loop, because the actual size of the loop to be swept by the [0 1 0] segment is much larger in that case. The difference comes from the fact that the ½⟨1 1 1⟩ loop is freely glissile (within MD timeframe) and therefore it adjusts the optimum interaction geometry with the approaching dislocation, while a ⟨1 0 0⟩ loop is immobile (at least at the MD timescale), therefore its initial position with respect to the DGP determines the junction configuration. As a result, the high resistance of the [0 1 0] loop is observed only at low temperature. Above 300 K, the flip of the upper part occurs spontaneously resulting in the absorption reaction. A critical stress of ~50 MPa is needed to accommodate the absorbed loop into a superjog and reform its shape to become glissile.

(c) The interaction details for the [0 0 1] loop are presented in figure 5 (see also animated gif figure 5 stacks.iop.org/JPhysCM/26/165402/mmedia). The dislocation approaches the loop (see figure 5(*a*)), makes a short ½ [1 1 $\bar{1}$] segment at the closest corner A (see figure 5(*b*)) and then at the corner C (see figure 5(*c*)). Thus, the dislocation arms pinned at the corners are linked by the ½[1 1 1] segment laying across the loop surface. Further load leads to the formation of a screw dipole. In the reaction at 150 K, the loop is simply sheared without cross-slip movement of the dipole arms. While at T = 300 K, one of the screw arms double cross-slips (i.e. up and down along 'AD' and 'DC' sides of the loop, see figure 5(*c*)), thereby converting the lower part of the loop into ½ [$\bar{1}$ $\bar{1}$ 1] orientation. The formed configuration is stable and immobile (because the upper part has [0 0 1] orientation), while the jogged dislocation glides away. Even though the interaction mechanism changes with temperature, the unpinning of the dislocation always requires the formation of the screw dipole, and therefore τ_C stays nearly constant in the

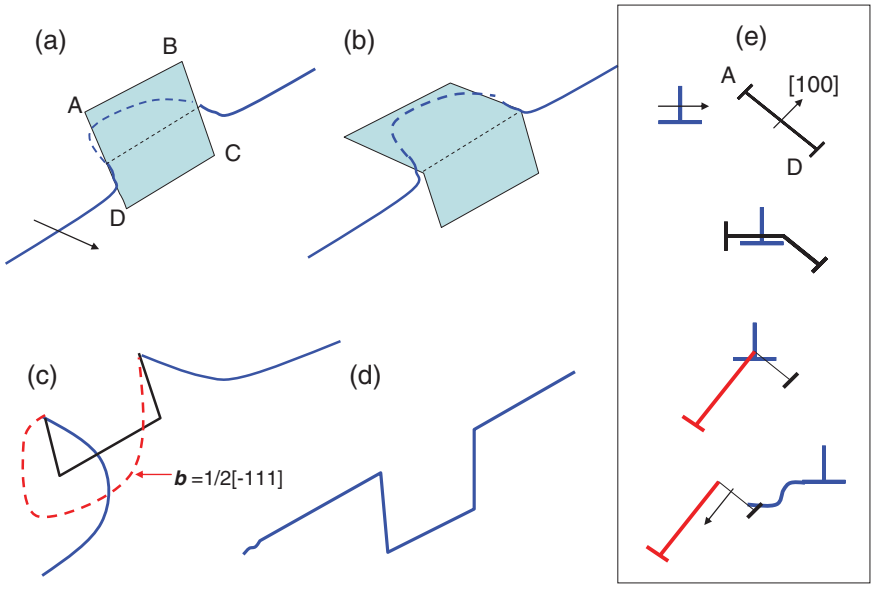

Figure 3. Schematic representation of the interaction mechanism for a loop with $\boldsymbol{b}_L = [1\,0\,0]$ at intermediate temperature, $T = 300$–600 K.

temperature range 150–600 K. At $T = 800$ K, the complete absorption of the loop occurs by the flip of the upper part and sequential interaction with the ½[1 1 1] and [0 0 1] segments of the dislocation and loop, respectively.

Based on the compilation of reactions presented above, one can note the intimate relation between the interaction geometry and absorption mechanism. The loops with $\mathbf{b}_L$ inclined to the DGP are absorbed by the 'flip' of their upper half, which is equivalent to the dissociation reaction: $[100] = ½[111] + ½[\bar{1}11]$. Apparently, the dissociation is induced by the external stress imposed from the approaching dislocation line. Another possibility is the direct propagation of a ⟨100⟩ segment along the loop surface. In the reactions involving loops with BV belonging to the DGP, the loop absorption requires first the emergence of a screw dipole and is completed by the cross-slip movement of screw arms. We can therefore reveal the following three principal mechanisms triggering the absorption: (1) dissociation of a ⟨100⟩ segment; (2) glide of a ⟨100⟩ segment across the loop surface; (3) cross-slip movement of a ½⟨111⟩ screw segment along ⟨100⟩ sides of the loop.

In the absence of C atoms, three basic reaction mechanisms (RM) can be distinguished, depending on the interaction geometry and simulation temperature:

(RM#1) Loop shear without cross-slip, which occurs for loops with BV = [1 0 0] and [0 0 1] at the lowest temperature studied (i.e. 150 K).

(RM#2) Formation of a screw dipole, local cross-slip around a loop, unpinning resulting in the formation of a 'bi-loop'. This RM operates in the intermediate temperature range (300–600 K) for loops with BV = [1 0 0] and [0 0 1].

(RM#3) Flip of the upper part and complete absorption on dislocation line, taking place for the [0 1 0] loop in the intermediate temperature range, and for all loops at 800 K and above.

Having these mechanisms and temperature limits in mind, we have studied the effect of carbon decoration. Carbon atoms are expected to segregate in the tensile regions of the dislocations, as has been revealed in our early study, particularly for ⟨100⟩ edge dislocations and loops [31]. The presence of carbon atoms directly in the loop core imposes a certain disturbance of its equilibrium structure and therefore may modify or suppress any of the three above listed principal mechanisms involved in the absorption process, and as a result may change the whole reaction mechanism.

3. Brief summary of computational details

As in our preceding works [28–30], the simulation scheme of a periodic array of dislocations developed in [32] is employed. The principal axes x, y and z of the simulated bcc crystal, as shown in figure 1, are oriented along the [1 1 1], [1 1 $\bar{2}$] and [$\bar{1}$ 1 0] directions, respectively. The edge dislocation with BV= 1/2[1 1 1] and slip plane x–y is created along the y direction with periodic boundary conditions applied along the x and y axes. The box is divided into three parts along z, so that the upper and lower parts (consisting of several atomic planes) contain rigidly fixed atoms. A glide force in the x direction on the dislocation is generated by the relative displacement of the rigid blocks in the x direction, which corresponds to simple shear strain e_{xz}. The resolved shear stress is calculated as $\tau = F_x/A_{xy}$, where F_x is the total force in the x direction on the lower outer block from all atoms in the inner region and A_{xy} is the x–y cross-section area of the box.

The inner region of the MD box was contained 101×3 non-equivalent atomic planes along x, 30×6 along y and 25×2 along z (corresponding to $25 \times 21 \times 10\,\text{nm}^3$). Five different temperatures were simulated, namely: 150, 300, 450, 600 and 800 K. The lattice parameter was adjusted for each temperature to respect zero pressure condition. MD simulations were started by initializing the velocity of the relaxed atoms according to Maxwell's distribution for the desired simulation temperature. After thermalization, shear was applied

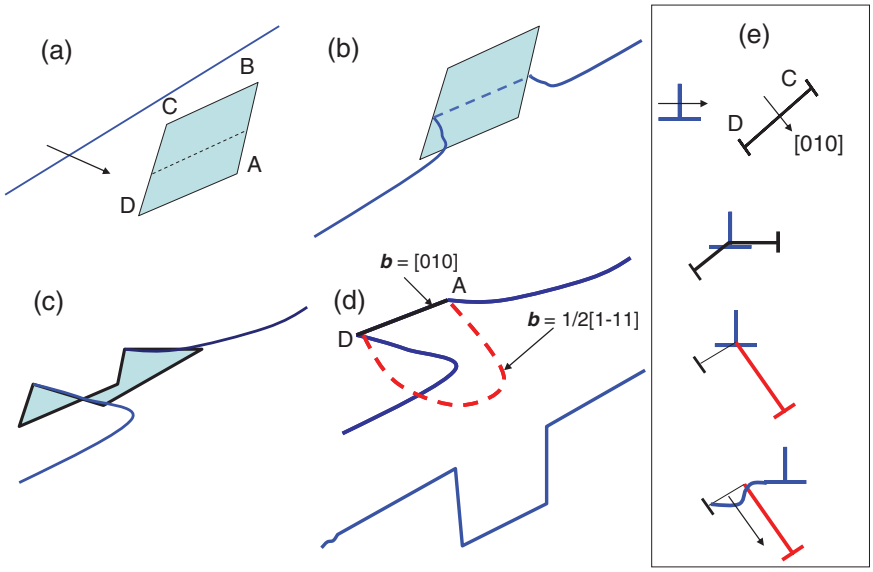

Figure 4. Schematic representation of the interaction mechanism for a loop with $\boldsymbol{b}_L = [0\,1\,0]$ occurring at $T \geqslant 150$ K.

at fixed strain rate, resulting in the dislocation velocity of 10 m s^{-1} determined using Orowan's law [6]. The integration of Newton's equations was performed using a constant time step (2 fs) in the microcanonical NVE ensemble, in which a number of particles, system volume and total energy are conserved if the work of external forces is taken into account. No temperature control was applied, as the temperature increase within a typical simulation run was negligible.

All simulations used a recently developed covalent bond many-body interatomic potential for the Fe–C system [33]. This potential removes most of the shortcomings of previously developed Fe–C potentials and provides a correct (i.e. in line with *ab initio* data) trend for the energetics of vacancy–carbon (covalent directional bonding), C–⟨1 1 0⟩ self-interstitial and C–C complexes in a bcc Fe matrix. Another reason to apply this potential is that it is the only available Finnis–Sinclair-type potential that includes the C–C interaction. The Fe–Fe part of this potential, derived by Ackland *et al* [34] predicts the compact core structure for a ½⟨1 1 1⟩ screw dislocation in agreement with *ab initio* calculations.

Visual inspection of dislocation configurations formed during the simulated reactions was performed by identifying atoms belonging to dislocation cores. We used the analysis specially developed for high temperature simulations in [17, 18], that combines different properties of core atoms, namely: atomic disregistry, coordination number, common neighbours and potential energy.

An interstitial dislocation loop of square shape with sides oriented along ⟨1 0 0⟩ directions was placed so that its centre coincided with the DGP. The loop had a size of ~3.5 nm. Three possible orientations for the loop BV ([1 0 0], [0 1 0] and [0 0 1]) were introduced. To study the effect of different level of carbon segregation, we have studied four possible carbon arrangements, including from one to four C atoms. In all cases, these were placed in the middle of the loop's sides, in the most favourable position (tensile dislocation core region), as defined in our earlier study [31]. Pairs of C atoms were placed on opposite (up–down or left–right) and adjacent (up–right or left–down) sides. Two configurations were generated for a triplet of C atoms, placing the impurities on left–up–right and left–down–right sides. Correspondingly, four configurations were inspected for an isolated C atom. For each interaction geometry (3 variants) and each simulation temperature (5 variants) 11 different C atom arrangements were inspected, which sums up to a total of 165 reactions.

When inspecting the RMs, we found that it was the same for configurations containing three and four C atoms, hence we did not distinguish the results. In the other cases, the RMs differ for the configurations where C atoms were placed on the sides below or above the glide plane. The reasons for these effects will be discussed later. To reduce the number of plots and figures presented, we subdivided the results by grouping configurations leading to the qualitatively (and very often quantitatively) same results. For a single C atom, we distinguish configurations in which the atom is below and above the DGP and refer to them as 'DN' and 'UP', respectively. For pairs of C atoms, we distinguish configurations in which C atoms are placed on the upper and lower sides (referred to as 'UD') and left and right sides (referred to as 'LR'). The same notation will be used to report the unpinning stress (averaged over the total number of configurations of that type).

4. Results

The results have shown that carbon decoration changes the interaction mechanism mostly in the reactions modelled in the intermediate temperature range, and mainly involving loops with BV [1 0 0] and [0 0 1]. The absorption reaction is always observed for the [0 1 0] loop irrespective of temperature and number of decorating C atoms. As the interaction mechanism modifies, the unpinning stress changes as well and usually increases. Generally, the unpinning stress increases with the number of decorating C atoms. To rationalize the interrelation

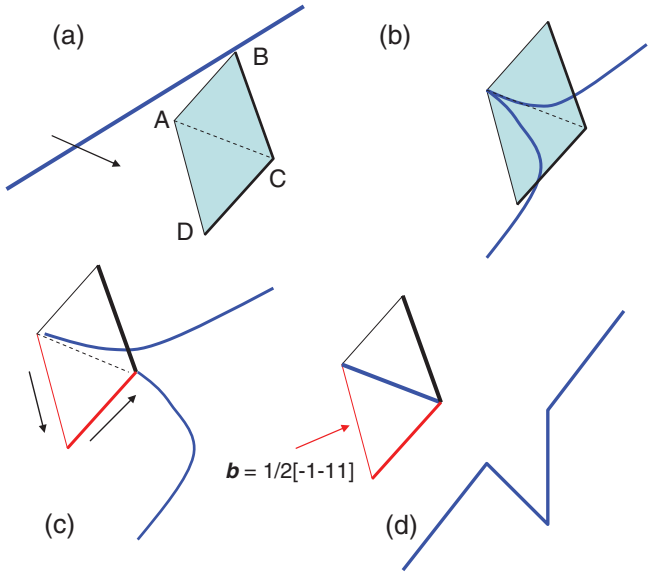

Figure 5. Schematic representation of the interaction mechanism for a loop with $\boldsymbol{b}_L$= [0 0 1] in the intermediate temperature range T =300–600 K.

between the unpinning stress increase and carbon decoration, we first discuss its impact on the interaction mechanisms.

4.1 Effect of carbon decoration on the interaction mechanisms

In addition to the three mechanisms revealed in pure Fe, two more types of reactions were observed for the decorated loops. The fourth RM (henceforth referred to as RM#4) was found to operate for the loops with BV [1 0 0] and [0 0 1]. A sequence of snapshots is given in figure 6 (see also animated gif figure 6. in the online supplementary material stacks.iop.org/JPhysCM/26/165402/mmedia) for the reaction involving the [1 0 0] loop decorated by four C atoms. The interaction proceeds in the same way as in pure Fe (see figure 3 and its description in section 2) up to the point when the upper part of the loop flips on the DGP (see figure 6(*c*)). After that the propagation of the [1 0 0] segment downwards across the loop surface does not occur and the screw dipole closes instead. As a result, a ½[$\bar{1}$ 1 1] loop is left behind (see figure 6(*d*)). Since the upper part was partially absorbed on the dislocation line, the reformed ½[$\bar{1}$ 1 1] loop has a size of ~2 nm (i.e. 1.5 times smaller than the original [1 0 0] loop). Two out of four C atoms remain attached to the core of the reformed loop, while the other two (previously attached to the dissociated segments) are free to migrate in the matrix.

As a demonstration of the effect of carbon decoration on the stress–strain relationship (τ–ε), we present the corresponding curve in figure 7, compared with that for the undecorated loop (which was completely absorbed), simulated under the same conditions. Clearly, the suppression of the absorption reaction leads to a higher unpinning stress (more than double), as expected since the closure of a screw dipole requires the highest stress. In principle, the above described mechanism can be considered as a subtype of RM#3, in which the last stage (propagation of the RS across loop surface) was suppressed. Once the resolved shear stress reached a critical value screw dipole closure naturally took place.

The second additional mechanism (henceforth referred to as RM#5) revealed for the decorated loops was seen only for the [0 0 1] loops in simulations at T = 450 and 600 K. The visualization snapshots in figure 8 show the reaction at T = 450 K for the loop decorated by two C atoms placed on sides AD and DC. The latter two are the sides along which the cross-slip movement takes place if the temperature regime corresponds to RM#2 (see its description in section 2). The initial stage of the interaction is the same as in RM#2, but the reaction ceases at the step involving the cross-slip movement (see figure 8(*b*)). Applying sufficiently high shear stress the cross-slip activates, but unlike in the absence of the decoration both arms encircle the loop. The closest arm goes from the corner A to C via D, while the furthest arm cross-slips up to the corner B and then down to C. The configuration at the end of the cross-slip movement is shown in figure 8(*c*). As a result, the loop is converted into ½[1 1 $\bar{1}$] orientation and partially absorbed by the dislocation line (see figure 8(*d*)). Importantly, the two C atoms are displaced during the cross-slip movement and the reformed ½[1 1 $\bar{1}$] loop is free to migrate. The critical stress in the case of the above described RM (curve not shown) was about 25% higher than that obtained for the undecorated loop.

To provide a general picture about the effect of carbon decoration on the interaction mechanism, we have constructed histograms for the [1 0 0] and [0 0 1] loops showing the number of RM as a function of temperature. The height of the columns in figure 9 corresponds to the number of RM introduced in sections 2.1 and 4.1. It is clear that RM are not affected at the highest temperature, as thermal activation eventually compensates for the C-added resistance.

The main modifications occur in the temperature range 300–600 K. In the case of the [1 0 0] loop, decorating C atoms suppress the complete absorption and change mechanism to the formation ½[$\bar{1}$ 1 1] loop, which emerges after the unpinning.

In the case of the [0 0 1] loops, C atoms, placed on the loop sides subject to the interaction with the cross-slipping screw arms, eventually increase the critical stress for the propagation of the screw segments. At a higher level of stress, the activation of the cross-slip movement of both dislocation arms becomes possible (which was never seen for undecorated loops). As a result, the whole loop can be converted into ½[1 1 $\bar{1}$] orientation. Hence, the C decoration biases the interaction mechanism towards the transformation from ⟨1 0 0⟩ into ½⟨1 1 1⟩ type, instead of leading to the complete absorption into a glissile superjog. Notably, the decoration of at least two sides of the loops is necessary to modify the reaction mechanism.

We also stress that in reactions modelled at elevated temperature, C atoms were regularly detached from the loops after the interaction. By tracing the coordinates of the C atoms, it appeared that their movement took place simultaneously with the reformation of the loop's segments entering the reactions with the gliding dislocation. The limited C migration (and release from the loops) could therefore serve as indication of irreversible dislocation–loop interaction, modifying the original structure of the loops.

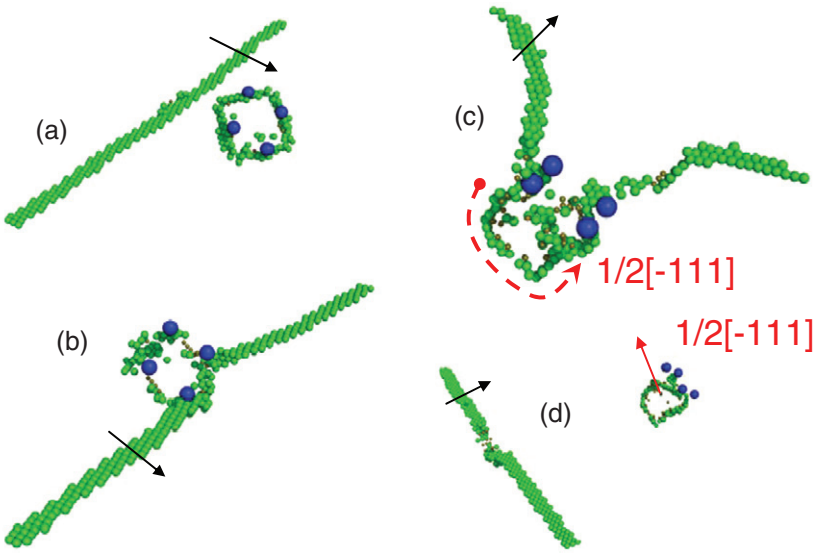

Figure 6. Visualization of different stages of the reaction involving a [1 0 0] loop decorated by four C atoms (blue spheres) at $T = 300$ K. A black arrow shows the direction of dislocation movement. On (*d*), the dislocation got unpinned and transmitted to the left part of simulation box via periodic boundary conditions. A red dashed line shows the position of the ½[$\bar{1}$ 1 1] segment formed after the flip of the upper part of the pre-existing [1 0 0] loop.

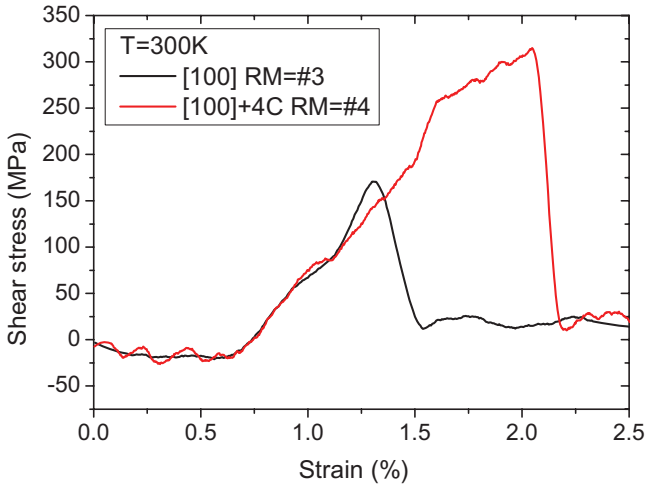

Figure 7. τ–ε plots for reactions with undecorated and decorated (by 4 C atoms) [1 0 0] loop simulated at $T = 300$ K.

4.2 Effect of carbon decoration on unpinning stress

The values of the unpinning stress measured in all the simulated reactions are summarized in figure 10, and the results for undecorated loops (obtained in [17, 30]) are also added. The error bars on the curves for undecorated loops were obtained from the five runs for each interaction geometry and temperature. In the calculations involving C atoms each point is averaged over two runs, which brings a considerable scattering and makes the comparison somewhat ambiguous. Despite that, it is possible to reveal at least two effects of carbon decoration on τ_C:

(i) even though carbon decoration does not affect the RM for the [0 1 0] loops, the unpinning stress is regularly higher for the decorated loops (see figure 10(*b*)) in the temperature range 300–600 K.

(ii) There is considerable (and reproducible for different carbon arrangements) increase of τ_C for the [1 0 0] and [0 0 1] loops at $T = 300$–450 K, at which the decoration modifies the interaction mechanisms, suppressing loop absorption.

Thus, carbon decoration leads to the increase of the loop strength, at least in the intermediate temperature interval. In simulations at the lowest and highest temperatures (i.e. 150 and 800 K), the effect of carbon on the unpinning stress is unclear, due to a large scatter of the results. Clearly, a better statistic is necessary to establish more robust and meaningful comparison.

5. Discussion

The results for the ⟨1 0 0⟩ interstitial loops decorated by C atoms presented here reveal clearly that the decoration affects the RM and increases the unpinning stress. Even though we have studied the interaction with the gliding ½[1 1 1]($\bar{1}$ 1 0) edge dislocation only, the mechanisms due to which the modification of the RM and unpinning stress takes place will also operate for ½⟨1 1 1⟩ screw dislocations, and edge dislocations gliding in ⟨1 1 2⟩ planes. Hence, the decoration is expected to affect the interaction of loops with moving dislocations of different characters in both ⟨1 1 0⟩ and ⟨1 1 2⟩ slip planes.

The most pronounced and reproducible increase of the unpinning stress for the decorated loops was found in the intermediate temperature range from 300 up to 600 K. In the case of the [1 0 0] and [0 1 0] loops, the increase of τ_C clearly correlates with the modification of the interaction mechanism, which explains its origin. In the case of the [1 0 0] loops, at a certain stage of the interaction, the C atoms suppress the propagation of the [1 0 0] segment across the loop surface, which otherwise

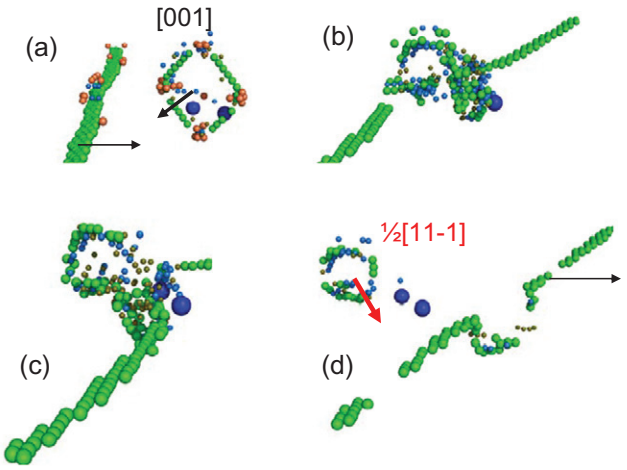

Figure 8. Visualization of different stages of the reaction involving a [0 0 1] loop decorated by 2 C atoms (blue spheres) simulated at 450 K. On (*d*), the jogged dislocation got unpinned, leaving behind a ½[1 1 $\bar{1}$] loop.

occurs in reactions with undecorated loops (see figure 4(*d*)). This prevents complete loop absorption and simultaneously changes the unpinning reaction pathway, resulting in the emergence and closure of a screw dipole. Since the propagation of the [1 0 0] segment completing the reaction is to occur downwards, the effect is therefore seen in configurations with C atoms placed below the DGP.

In the case of the [0 0 1] loop, the presence of C atoms on the loop's segments enhances their resistance against propagation of screw arms (i.e. step 'c' in figure 5) and therefore delays the unpinning. It is important, for this to happen, that a C atom should be encountered by the propagating screw segments. If a sufficient number of C atoms is placed on the relevant loop sides, the resolved shear stress may reach a critical value at which an alternative mechanism, not observed without decoration, activates. That situation realizes in the case of 3C and 4C decoration of the [0 0 1] loop at 450–600 K (see description of RM#5 in section 4.1) which leads to the modification of the reaction outcome.

Finally, in the case of the 'weak' [0 1 0] loops, the addition of an increasing number of C atoms in the loop core led to the reproducible increase of the unpinning stress. In that configuration, it was essential that C atoms should be placed on the 'left' and 'right' sides (i.e. AB and CD in figure 1), across which the [0 1 0] segment has to propagate to complete the reaction. The retention of its movement due to the extra resistance offered by decorating C atoms explains the added strengthening. Correspondingly, strong effect was observed for the 'LR' pair and configurations involving three and four C atoms.

One can therefore conclude that the actual level of carbon segregation is an important parameter defining both the loop's strength (i.e. hardening) and RM (i.e. plastically induced modification of microstructure). The results presented here, together with our previous studies [28–30] that address the effect of chromium and carbon decoration, have clearly demonstrated that the disturbance of the loop core by impurity inclusion suppresses certain dislocation-mediated mechanisms that determine the whole reaction process. As a result, it may lead to increase of τ_C, may modify the reaction outcome, or provoke both effects. These parametric and self-consistent studies involving both ½⟨1 1 1⟩ and ⟨1 0 0⟩ loops therefore confirm unambiguously that impurity/solute segregation on radiation defects is another variable (in addition to deformation temperature and rate) that influences local deformation mechanisms and in turn causes global changes of microstructure under plastic deformation. It therefore implies that not only the density and the size distribution of defects, but also their microchemical morphology can be a valuable input from microstructural predictive models embedded in the multi-scale chain of computational tools [35]. At the same time, whether or not the specific mechanisms described here will be of relevance in real situations will depend on the frequency of ⟨1 0 0⟩ loops and carbon decoration. Since the appearance of these loops is favoured at higher temperature (at least upon ion irradiation), it is possible that the enhancement of their strength as dislocation obstacles is not practically measurable, but the main message is that the increase of obstacle strength as a consequence of solute segregation on loops is a general phenomenon, independent of loop type.

The so far identified effects of Cr and C segregation have very similar qualitative consequences: (i) suppression of loop absorption and (ii) increase of τ_C. However, these two experimentally observed segregating atoms [26, 27] exhibit significantly different features. Cr atoms are substitutional solutes. The spatial rearrangement of Cr atoms on a loop in the course of interaction with dislocations is therefore naturally not possible in the case of standard mechanical tests (and of course in MD simulations) as it requires defects offering the possibility of mass transport (e.g. vacancies). Carbon atoms, on the other hand, are interstitial impurities, which perform in-core diffusion at sufficiently high temperature. In the high temperature simulations carried out here, we have regularly observed limited, but non-negligible, carbon migration. This is a very important feature and should be regarded as a fundamental difference in the way Cr and C atoms influence loops' strength. The decorating C atoms are often detached from the loops after dislocation unpinning, in most of the reactions, especially in simulations at $T \geq 450$ K. In agreement with the present observations, previous works addressing the mobility of carbon decorating dislocations loops also reported limited carbon migration occurring within a relatively short MD-timescale frame [29]. This implies that local carbon in-core rearrangement is certainly expected to take place in the reactions involving slowly moving dislocations (for velocities much lower than metres per second, unachievable for MD techniques) in the technologically important temperature range. How strongly the 'pipe migration' of carbon would influence RM and unpinning stress remains to be investigated. It is obvious, however, that standard MD techniques are not applicable for this problem: the further development of large-scale accelerated dynamics or hybrid MD–Monte Carlo approaches is necessary.

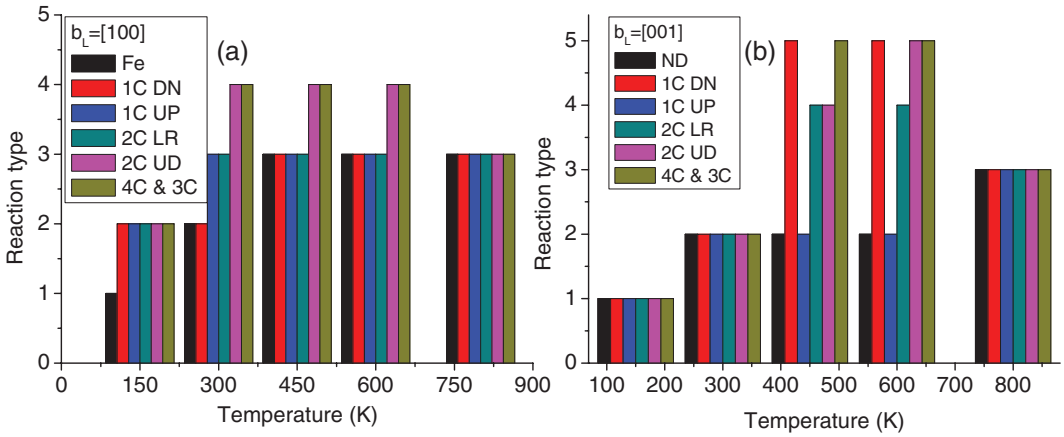

Figure 9. Classification of reaction mechanisms as a function of temperature and level of carbon enrichment.

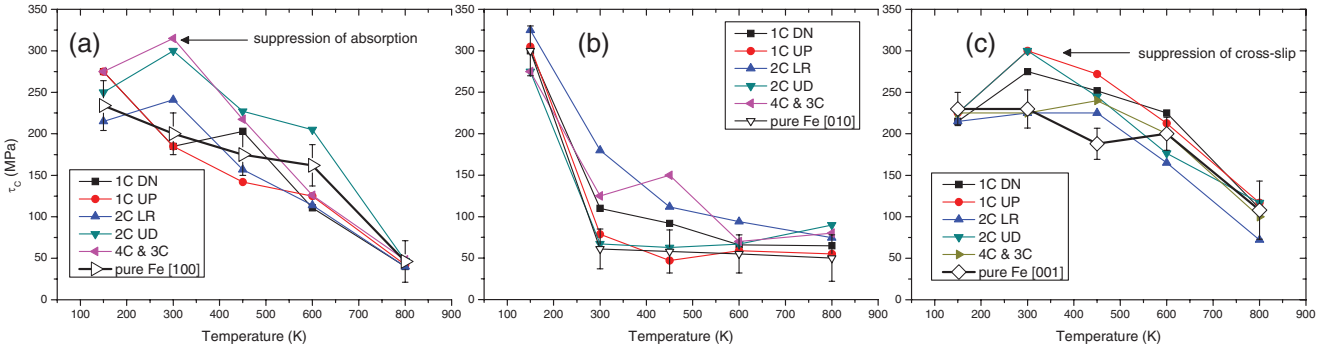

Figure 10. The unpinning stress as a function of temperature calculated for (*a*) [1 0 0], (*b*) [0 1 0] and (*c*) [0 0 1] loops with and without carbon decoration.

6. Conclusions

Based on the above presented results and their discussion the following conclusions are drawn:

(i) Carbon decoration leads to the modification of the reaction mechanism in the intermediate temperature range (300–600 K), and it is expressed in the suppression of complete absorption of $\langle 1\,0\,0\rangle$ loops in favour of transformation into $\frac{1}{2}\langle 1\,1\,1\rangle$ loops. The effect of carbon decoration on the interaction mechanism enhances with increasing number of C atoms residing on the core of the dislocation loop.

(ii) There is a reproducible increase of the unpinning stress for the decorated loops in the temperature interval T=300–600 K. The reasons for the higher loop resistance are rationalized in terms of the modification and suppression of several elementary dislocation reactions contributing to the [1 0 0] loop–dislocation interaction process.

(iii) The strongest effect of carbon decoration on the loop resistance is seen for the 'weak' [0 1 0] loops, which otherwise are athermally absorbed on dislocation lines at T = 300 K and above.

(iv) Non-negligible carbon migration was regularly observed in reactions at $T \geq 450$ K. This implies that carbon rearrangement is expected to take place in the course of the loop–dislocation interaction at elevated temperature and low deformation rates. The effect of in-pipe carbon diffusion on the reaction mechanism and unpinning stress should therefore be investigated.

Acknowledgments

This work, supported by the European Commission under the Contract of Association between EURATOM/SCK-CEN, was carried out within the framework of the European Fusion Development Agreement. Partial support was also received from the EURATOM 7th framework programme, under Perform 60 project. DT thanks his colleague Dr. L. Malerba for the useful remarks and proofreading.

References

[1] Klueh R L and Nelson A T 2007 *J. Nucl. Mater.* **371** 37
[2] Lucon E and Vandermeulen W 2009 *J. Nucl. Mater.* **386–388** 254
[3] Lucon E, Leenaers A and Vandermeulen W 2008 *Fusion Eng. Design* **83** 620
[4] Tong Z and Dai Y 2009 *J. Nucl. Mater.* **385** 258
[5] Bacon D, Gao F and Osetsky Y 2000 *J. Nucl. Mater.* **276** 1
[6] Hull D and Bacon D J 2001 *Introduction to Dislocations* (Oxford: Butterworth-Heinemann)
[7] Gelles D and Schaeublin R 2001 *Mater. Sci. Eng.* **309–310** 82
[8] Zinkle S J and Singh B N 2006 *J. Nucl. Mater.* **351** 269
[9] Gaganidze E, Schneider H, Dafferner B and Aktaa J 2006 *J. Nucl. Mater.* **355** 83

[10] Matijasevic M and Almazouzi A 2008 *J. Nucl. Mater.* **377** 147
[11] Matjiasevic M, Lucon E and Almazouzi A 2008 *J. Nucl. Mater.* **377** 101
[12] Was G S 2007 *Fundamentals of Radiation Materials Science* (New York: Springer)
[13] Nomoto A, Soneda N, Takahashi A and Ishino S 2005 *Mater. Trans.* **46** 463
[14] Bacon D, Osetsky Y and Rong Z 2006 *Phil. Mag.* **86** 3921
[15] Terentyev D, Malerba L, Bacon D and Osetsky Y 2007 *J. Phys.: Condens. Matter* **19** 456211
[16] Liu X Y and Biner S B 2008 *Scr. Mater.* **59** 51
[17] Terentyev D, Grammatikopoulos P, Bacon D and Osetsky Y 2008 *Acta Mater.* **56** 5034
[18] Terentyev D, Bacon D J and Osetsky Y N 2010 *Phil. Mag.* **90** 1019
[19] Terentyev D, Osetsky Y N and Bacon D J 2010 *Scr. Mater.* **62** 697
[20] Terentyev D A, Osetsky Y N and Bacon D J 2010 *Acta Mater.* **58** 2477
[21] Terentyev D, Monnet G and Grigorev P 2013 *Scr. Mater.* **69** 578
[22] Arsenlis A, Rhee M, Hommes G, Cook R and Marian J 2012 *Acta Mater.* **60** 3748
[23] Porollo S, Dvoriashin A, Vorobyev A and Konobeev Y 1998 *J. Nucl. Mater.* **256** 247
[24] Katoh Y, Kohyama A and Gelles D 1995 *J. Nucl. Mater.* **225** 154
[25] Jenkins M L, Yao Z, Hernandez-Mayoral M and Kirk M A 2009 *J. Nucl. Mater.* **389** 197
[26] Terentyev D, Klimenkov M and Malerba L 2009 *J. Nucl. Mater.* **393** 30
[27] Jiao Z and Was G S 2011 *Acta Mater.* **59** 4467
[28] Terentyev D, Bergner F and Osetsky Y O 2012 *Acta Mater.* **61** 1444
[29] Terentyev D, Anento N and Serra A 2012 *J. Phys.: Condens. Matter* **24** 455402
[30] Terentyev D and Bakaev A 2013 *J. Phys.: Condens. Matter* **25** 265702
[31] Terentyev D, Anento N and Serra A 2012 *J. Nucl. Mater.* **420** 9
[32] Osetsky Y N and Bacon D J 2003 *Modelling Simul. Mater. Sci. Eng.* **11** 427
[33] Hepburn D and Ackland G 2008 *Phys. Rev.* B **78** 165115
[34] Ackland G, Mendelev M, Srolovitz D, Han S and Barashev A 2004 *J. Phys.: Condens. Matter* **16** 1
[35] Wirth B, Odette G, Marian J, Ventelon L, Young-Vandersall J and Zepeda-Ruiz L 2004 *J. Nucl. Mater.* **329–333** 103